

Accepted Manuscript

A novel AIE chemosensor based on quinoline functionalized Pillar[5]arene for highly selective and sensitive sequential detection of toxic Hg^{2+} and CN^-

Xiao-Qiang Ma, Yun Wang, Tai-Bao Wei, Li-Hua Qi, Xiao-Mei Jiang, Jin-Dong Ding, Wen-Bo Zhu, Hong Yao, You-Ming Zhang, Qi Lin

PII: S0143-7208(19)30010-5

DOI: <https://doi.org/10.1016/j.dyepig.2019.01.049>

Reference: DYPI 7322

To appear in: *Dyes and Pigments*

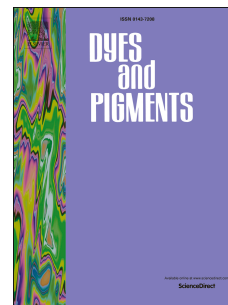
Received Date: 3 January 2019

Revised Date: 28 January 2019

Accepted Date: 28 January 2019

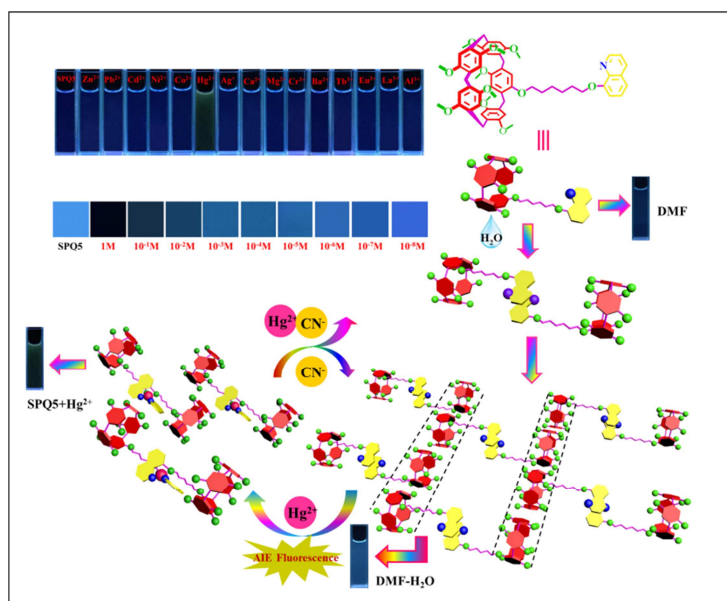
Please cite this article as: Ma X-Q, Wang Y, Wei T-B, Qi L-H, Jiang X-M, Ding J-D, Zhu W-B, Yao H, Zhang Y-M, Lin Q, A novel AIE chemosensor based on quinoline functionalized Pillar[5]arene for highly selective and sensitive sequential detection of toxic Hg^{2+} and CN^- , *Dyes and Pigments* (2019), doi: <https://doi.org/10.1016/j.dyepig.2019.01.049>.

This is a PDF file of an unedited manuscript that has been accepted for publication. As a service to our customers we are providing this early version of the manuscript. The manuscript will undergo copyediting, typesetting, and review of the resulting proof before it is published in its final form. Please note that during the production process errors may be discovered which could affect the content, and all legal disclaimers that apply to the journal pertain.



Graphical Abstract

Xiao-Qiang Ma^a, Yun Wang^a, Tai-Bao Wei^{a*}, Li-Hua Qi^a, Xiao-Mei Jiang^a, Jin-Dong Ding^a, Wen-Bo Zhu^a, Hong Yao^a, You-Ming Zhang^{a,b} and Qi Lin^{a*}



A novel 8-hydroxyquinoline functionalized pillar[5]arene (SPQ5) with AIE fluorescence could sequentially detect toxic Hg^{2+} and CN^- in aqueous medium with high selectivity and sensitivity.

A Novel AIE Chemosensor Based On Quinoline Functionalized Pillar[5]arene for Highly Selective and Sensitive Sequential Detection of Toxic Hg^{2+} and CN^-

Xiao-Qiang Ma^a, Yun Wang^a, Tai-Bao Wei^{a*}, Li-Hua Qi^a, Xiao-Mei Jiang^a, Jin-Dong Ding^a, Wen-Bo Zhu^a, Hong Yao^a, You-Ming Zhang^{a, b} and Qi Lin^{a*}

^a Key laboratory of Polymer Materials of Gansu Province, College of Chemistry and Chemical Engineering, Northwest Normal University, Lanzhou 730070, China.
E-mail: weitaibao@126.com, linqi2004@126.com

^b College of Chemistry and Chemical Engineering, Lanzhou City University, Lanzhou, Gansu, 730070, China.

ABSTRACT

Aggregation-induced emission (AIE) is widely used for fluorescence “on-off-on” detection ions and molecular. Herein, we report a novel AIE chemosensor through self-assembly of quinoline functionalized pillar[5]arene (**SPQ5**). The **SPQ5** can bind with Hg^{2+} tightly through coordinating reaction. By introducing Hg^{2+} into AIE-based chemosensor, metal-coordinated chemosensor (**SPQ5**- Hg^{2+}) was obtained, the **SPQ5**- Hg^{2+} could high selectively and sensitively detection of CN^- by competitive coordinating interactions. The LODs of **SPQ5** for Hg^{2+} and CN^- are 2.53×10^{-8} M and 7.71×10^{-8} M, respectively. In addition, Hg^{2+} test kit was prepared by loading the **SPQ5** chemosensor on a silica gel plate, which could more convenient and efficiency detection Hg^{2+} and CN^- . Interestingly, the chemosensor **SPQ5** could instant sense the Hg^{2+} and CN^- by the changing of fluorescence color and fluorescence intensity. Notably, the fluorescence intensity changes of **SPQ5** upon the addition of Hg^{2+} and CN^- were utilized as an IMP logic gate at the molecular level, using Hg^{2+} and CN^- as chemical inputs and the fluorescence intensity signal as the output. On the other hand,

the test kit by loading **SPQ5** on a silica gel plate was prepared for convenient detection of Hg^{2+} . This study provides a practical application for the sensing of toxic ions in aqueous solution by the construction of supramolecular system.

Keywords: Toxic ion; AIE fluorescence; Pillar[5]arene; Chemosensor; Highly sensitive detection; Logic gate.

1. Introduction

In recent years, detection of toxic ions has gained paramount importance in biological, chemical and environmental applications. Among the various cations and anions, mercury and cyanide are considered to be toxic ions for human health and natural environment. Mercury is one of the well-known heavy toxic metal which can exist in different forms, such as elemental, organic and inorganic forms [1-2]. The risk of such pollutants even at invisible trace level is that they can be progressively concentrated through the food chain and form a threat to human health. Moreover, low concentration of mercury induces wide variety of serious health effects. Similarly, CN^- is considered as one of the most toxic anions due to CN^- could associated with binding to the iron in hemoglobin, which interrupts electron transport and causes hypoxia [3-4]. In spite of its extreme toxicity, the CN^- is still extensively used in the gold and silver mining industry, plastic manufacturing and resin industry. Therefore, the quantitative detection of toxic ions are important area of ions detection research.

Chemosensors for sequential detection of diverse cations and anions, such as anion-anion [5-6], anion-cation [7-8], cation-anion [9-11], cation-cation [12-13], has been reported. An example of the sequential detection toxic ions via a single fluorescent chemosensor has been little reported to date. Additionally, development of selective and sensitive probes with environmental interest for the determination and visualization of analytes (metal ions [14-16], anions [17-19] and molecular [20-22]) is a very attractive research topic in the chemosensors [23-24]. A various of analytical methods has been reported [25-29] for detection of Hg^{2+} and CN^- , but the

fluorescence based technique is always attractive because of their high sensitivity, sensitive response time, and simple technology. The 8-hydroxyquinoline moiety has valuable structural characteristics of the most widely employed molecular platforms to construct many unique ionophoric systems for the recognition of important metal ions and effective light-emitting devices [30-31]. In recently, quinoline-functionalized pillar[5]arene reported by others mainly was supplied in fields of detection for radioactive element [32] and gas adsorption [33]. However, 8-hydroxyquinoline functionalized pillar[5]arene with AIE for detection of toxic ions is rarely.

Aggregation-induced emission (AIE) is a fluorescent phenomenon that a molecule or molecular fragment exhibits enhanced fluorescence properties in the aggregated state, as results of restriction of intramolecular motions, rotations or vibrations, that led to the three-dimensional (3D) conformations of AIE gens effectively strengthened aggregated-state fluorescence [34-35]. Fluorescence based on AIE chemosensors have emerged to show great potential for chemical sensing [36-38], optoelectronic applications [39-41] and bio-imaging [42-44]. Construction of functional supramolecular polymer into AIE molecule can greatly expand their potential fluorescence sensing application [45-48]. In recent years, tetraphenylethene (TPE) has been vibrantly developed, due to TPE containing four rotatable phenyl rings exhibits AIE activity [49-51]. Additionally, triphenylamine [52-53] and 1, 8-Naphthalimide [54-56] derivatives are also receiving continuous attention owing to their wide AIE activity in ions detection and biological images.

Pillar[n]arenes as a new class of macrocyclic host have been widely reported due to their intrinsic uniquely rigid symmetrical pillar architecture and easy function

properties [57-59]. Pillar[5]arene-based various self-assembly driving forces such as hydrogen bonds [60-61], π - π stacking [62-63], host-guest interactions [64-65] and metal-ligand binding [66-67] C-H \cdots π interactions [68-69] and so on. Much more importantly, these various self-assembly driving forces also provide good opportunities to achieve controllable multi-stimuli response [70-71]. Developing a pillar[5]arene chemosensors based on AIE activity are always an important topic in this area. Therefore, they have obtained more and more attention of researchers in recent years. In our recent research, we found that pillar[5]arene-based supramolecular also reveal AIE activity [72-73].

In view of these and as a part of our research interests in ions recognition and pillar[5]arene-based supramolecular chemosensors [74-78], we report a novel 8-hydroxyquinoline functionalized pillar[5]arene fluorescent probe (**SPQ5**), which shown strong AIE fluorescence in aqueous solution. The **SPQ5** could act as an AIE-based chemosensor for highly selectivity and sensitivity detection of Hg^{2+} and CN^- in DMF/water (8:2, v/v) binary solution by coordination interaction. The LODs of **SPQ5** for Hg^{2+} is 2.53×10^{-8} M and CN^- is 7.71×10^{-8} M, respectively. Moreover, other cations and anions didn't interfere in the sensing processes. The Hg^{2+} sensing mechanism was based on coordination between Hg^{2+} and **SPQ5**, fluorescence recover by added CN^- due to CN^- break this coordination. In addition, Hg^{2+} test kits, prepared by loading the **SPQ5** on silica gel plates, could conveniently and efficiently detection of Hg^{2+} in aqueous solution with highly sensitivity. Meanwhile, we design IMP logic gate controlled by Hg^{2+} and CN^- can provide significantly increased the ability to expand the repertoire of available operations.

2. Experiment

2.1. Materials

Unless otherwise stated, all chemical reagents were obtained from commercial suppliers and used without further purification. Solvents used were purified and dried by standard methods prior to use. Commercially and were used without further purification. All the anions were added in the form of tetra butyl ammonium (TBA) salts, which were purchased from Sigmae Aldrich Chemical, stored in a vacuum desiccator. All cations were used as the perchlorate salts, which were purchased from Alfa Aesar and used as received.

Scheme 1

2.2. Instruments

Melting points were measured on an X-4 digital melting point apparatus and were uncorrected. Fluorescence spectra data were recorded on Shimadzu RF-5310 spectrometer. The NMR spectra were obtained on a Mercury-600 BB spectrometer with tetramethylsilane (TMS, δ scale with solvent resonances as internal standards) as inner standard. High-resolution MS was conducted on a Bruker Esquire 3000 Plus spectrometer (Bruker-Franzen Analytik GmbH Bremen, Germany) equipped with ESI interface and ion trap analyzer. Powder X-ray diffraction data were collected using a Rigaku RINT2000 diffract meter equipped (copper target; $\lambda = 0.154073$ nm). Scanning electron microscopy (SEM) images of the xerogels were investigated using JSM-6701F instrument.

2.2. Synthesis of **SPQ5**

Synthesis of **SPQ5**: Pillar[5]arene 2 (0.9 g, 1 mmol) and KI (0.183 g, 1.1 mmol) were added to a solution of K_2CO_3 (0.138 g, 1 mmol) and 8-hydroxyquinoline(0.16 g, 1.1 mmol) in acetone/N,N-Dimethylformamide (v/v 50:3). The mixture was heated under nitrogen atmosphere at reflux for 48 h. As shown in Scheme 2. The solid was filtered off and the solvent was removed. The crude product was isolated by column

chromatography using petroleum ether/ethyl acetate (v/v 5:1) to get a white solid **SPQ5** (0.61 g, 63%). m.p. 92-94°. ¹H NMR (Fig. S3) (600 MHz, CDCl₃, room temperature) δ (ppm): 8.95 (d, *J*=4Hz, 1H), 8.12 (t, *J*=8Hz, 1H), 7.45 (m, 2H), 7.38 (d, *J*=8Hz, 1H), 7.07 (d, *J*=6Hz, 1H), 6.78(m, 10H), 4.27 (d, *J*=8.3Hz, 2H), 3.86 (t, *J*=6Hz, 2H), 3.76 (d, *J*=10.5Hz, 10H), 3.66 (m, 27H), 2.10 (m, 2H), 1.86 (t, 2H), 1.64 (t, *J*=7.2Hz, 4H). ¹³C NMR (Fig. S4) (150MHz, CDCl₃, room temperature) δ (ppm): 155.04, 150.88, 150.84, 150.20, 149.54, 140.64, 136.11, 129.74, 128.57, 128.44, 128.36, 126.89, 121.76, 119.69, 115.01, 114.11, 140.01, 108.84, 69.03, 68.57, 55.91, 30.07, 29.55, 26.31. ESI-MS *m/z*: [**SPQ5**]⁺ Calcd C₅₉H₆₅N₁O₁₁ 964.17, found 964.46. (Fig. S5).

3. Results and discussion

A novel quinoline functionalized pillar[5]arene derivative (**SPQ5**) has been synthesized by rationally connected a pillar[5]arene moiety and an 8-hydroxyquinoline groups (Scheme 1). **SPQ5** and its intermediate were characterized by ^1H NMR and ^{13}C NMR, and ESI mass spectra (Fig. S1-S5). Interestingly, the **SPQ5** as novel AIE active moiety caused by pillar[5]arene shows strongly AIE fluorescence. In order to investigate the AIE influence, a series of aggregated fluorescence experiment were carried out (Fig. 1). The optical measurements of **SPQ5** were conducted in DMF/ H_2O (8:2, v/v) binary solution at a fixed concentration (2.0×10^{-4} M). The supramolecular chemosensor **SPQ5** has almost no fluorescence in pure DMF solution (Fig. 1). Upon the addition of various water content, the **SPQ5** exhibits enhanced aggregation fluorescence as water content increases and reaches the strongest emission intensity at $f_w = 20\%$, with the relative emission intensity (I/I_0) up to 7.88-fold at 410 nm (Fig. 1b). In the solution of **SPQ5**, white precipitate also appeared when water content increased over 40%. In addition, the AIE feature of **SPQ5** could be directly observed by the fluorescence color changes taken under 365 nm UV lamp (Fig. 1b, inset). The fluorescence quantum yields of **SPQ5** in pure DMF and DMF/water binary solution ($f_w = 20\%$) were determined as 11.24% and 37.8%, respectively, according to the corresponding formula [79], using quinine sulfate as standard.

Fig. 1

In order to further explore the AIE properties of **SPQ5**, XRD, Tyndall phenomenon

and SEM had been carried out. In the XRD spectra (Fig. S6), the powder of chemosensor **SPQ5** obtained from DMF had weakly signal peak. However, the powder obtained from DMF/H₂O (8:2, v/v) binary solution of **SPQ5** clearly shown significant pick at $2\theta = 23.25^\circ$ and $2\theta = 24.15^\circ$ ($d = 3.82 \text{ \AA}$ and 3.68 \AA). Above result attributed to enhancement of π - π stacking with increasing of water content. Interestingly, with increasing of the water content, especially when the water content reached 20%, a significant Tyndall phenomenon (Figure 2a) was observed in DMF/H₂O binary solution, indicating that the aggregation of **SPQ5** induced enhancement of AIE fluorescence. Meanwhile, after aggregation of **SPQ5** in DMF/H₂O binary solution, the surface morphology of **SPQ5** changed from irregular block (Fig. 6a) to coral-like structure (Figure 2a), which also indicates the formation of supramolecular polymers by aggregation of **SPQ5** in DMF/H₂O (8:2, v/v) binary solution, supporting the correctness of above self-assembly mechanism.

The AIE activity of chemosensor **SPQ5** was also investigated. By ¹H NMR titration methods, the aqueous-content-dependent ¹H NMR titration spectra (Fig. 3) provided important insights into their AIE behaviors, with the addition of D₂O, the hydrogen protons (H₂, H₃, H_{4,5}, H₆ and H₁) on the 8-hydroxyquinoline downfield 0.02, 0.03, 0.04, 0.03 ppm and upfield 0.03 ppm, respectively (Fig. 3), which could attributed 8-hydroxyquinolines moiety through π - π stacking interaction self-assembled into a supramolecular dimer. Meanwhile, the protons of aryl hydrogen of pillar[5]arene of cavity (Ha), chain alkyl(Hd), methoxy(Hc) and methylene hydrogen(Hb) upfield 0.01, 0.01, 0.03 and 0.02 ppm, respectively, indicated that a supramolecular network was

formed by π - π stacking between the cavities of the pillar[5]arene and driven by multiple C-H $\cdots\pi$ interactions between cavities of the pillar[5]arene and methoxy protons (Scheme 2c).

Fig. 2

The fluorescence behavior of **SPQ5** towards metal ions was carried out in DMF/H₂O (8:2, v/v) binary solution. The recognition profiles of the chemosensor **SPQ5** towards various cations (Zn²⁺, Pb²⁺, Cd²⁺, Ni²⁺, Co²⁺, Hg²⁺, Ag⁺, Ca²⁺, Mg²⁺, Cr³⁺, Ba²⁺, Tb³⁺, Eu³⁺, La³⁺ and Al³⁺) were primarily investigated using fluorescence spectra (Fig. 4), when 2.0 equiv. of the various cations were added, only Hg²⁺ could significantly quench the fluorescence, immediately. Meanwhile, blue fluorescence disappeared was observed under UV lamp (Fig. 4 Inset), the fluorescence intensity of the peak at 410 nm sharply decreased, which indicated that the chemosensor **SPQ5** changed into metal coordination polymer **SPQ5-Hg²⁺**. As a result, the Hg²⁺ could be easily detected through the fluorescent color of **SPQ5** solution transformation from blue to colorless under the UV lamp. The fluorescence spectral properties of chemosensor **SPQ5** towards Hg²⁺ were also carried out in the solution of DMF/H₂O (8:2, v/v), which we got the same experiment phenomenon as the above situation. In order to investigate the binding properties of the receptor **SPQ5** towards Hg²⁺, fluorescence titration of **SPQ5** has been carried out in DMF/H₂O (8:2, v/v) binary solution. As shown in Fig. S4, the spectral emission intensity of **SPQ5** quenched with the addition of Hg²⁺. In the fluorescence spectra, upon addition of increasing amounts of Hg²⁺ (0-1.73 equiv.) to the solution of **SPQ5** in DMF/H₂O (8:2, v/v), the

fluorescence emission at 410 nm showed a dramatic fluorescence quenching by 92% (quenching efficiency $(I-I_0)/I \times 100\% = 92\%$). The detection limit of the fluorescent spectra changes calculated on the basis of $3\sigma/S$ is 2.53×10^{-8} M for Hg^{2+} (Fig. S8), which is lower than other various reported methods (Table 1). The lower detection limit revealed the high sensitivity of **SPQ5** towards Hg^{2+} . In addition, when the amount of Hg^{2+} is beyond 1.73 equiv., the emission at 410 nm tends to saturation. Furthermore, in order to quantify the complexation ratio between **SPQ5** and Hg^{2+} , the Job's plot was conducted by varying the concentration of both **SPQ5** and Hg^{2+} (Fig. S9), the turning point appears at the mole fraction of 0.33 equiv. ($\text{Hg}^{2+}/\text{SPQ5-Hg}^{2+}$) indicates that **SPQ5** and Hg^{2+} formed a 2:1 complex.

Fig. 3

Moreover, the successive recognition property of **SPQ5** towards cations was further investigated by adding various cations (Zn^{2+} , Pb^{2+} , Cd^{2+} , Ni^{2+} , Co^{2+} , Ag^+ , Ca^{2+} , Mg^{2+} , Cr^{3+} , Ba^{2+} , Tb^{3+} , Eu^{3+} , La^{3+} and Al^{3+}) into **SPQ5-Hg²⁺** DMF/H₂O (8:2, v/v) binary solution. As a result, **SPQ5** could detect Hg^{2+} with specific selectivity and the addition of other cations have no effect on recognition performance (Fig. 5). Due to the **SPQ5** showing excellent “turn off” response to Hg^{2+} , we rationally introduced competitive coordination properties by adding Hg^{2+} into **SPQ5** to prepare **SPQ5-Hg²⁺**. Interestingly, **SPQ5-Hg²⁺** showed single guest-response properties, by adding various anions including F^- , Cl^- , Br^- , I^- , AcO^- , HSO_4^- , H_2PO_4^- , ClO_4^- , CN^- , SCN^- , N_3^- and OH^- (4 equiv.) into the solution of **SPQ5-Hg²⁺** in DMF/H₂O (8:2, v/v). For an instant, the **SPQ5-Hg²⁺** could selectively fluorescence “turn-on” sensor CN^- (Fig. S10).

In order to examine the efficiency between **SPQ5**- Hg^{2+} and CN^- , fluorescence emission titration experiment was monitored. In the fluorescence titration spectra, with an increasing amount of CN^- (0-4.8 equiv.), the fluorescence emission bands at 410 nm appeared gradually. (Fig. S11). Meanwhile, the fluorescence detection limit was calculated on the basis of $3\sigma/S$ is 7.71×10^{-8} M for CN^- by fluorescence titrations (Fig. S12), which indicates that **SPQ5**- Hg^{2+} could detect CN^- lower than previous reported [80-81]. To validate the selectivity of sensor **SPQ5**, the same tests were applied using F^- , Cl^- , Br^- , I^- , AcO^- , HSO_4^- , H_2PO_4^- , ClO_4^- , SCN^- , N_3^- and OH^- (4 equiv.). None of these anions induced any significant changes in the fluorescent spectrum of the sensor progress (Fig. S13). From the bar diagram, we could easily consider that the effects on emission intensity of **SPQ5**- Hg^{2+} and CN^- aqueous solutions upon addition of various anions were almost negligible. Therefore, it was clear that other anions didn't interfere during the detection of CN^- .

Fig. 4

This fluorescence “on-off-on” phenomenon was induced by the competitive coordination of Hg^{2+} and CN^- . The Hg^{2+} competitive coordination with CN^- lead to the fluorescent of **SPQ5** solution recovered. Therefore, the solution of **SPQ5**- Hg^{2+} could “turn on” sense CN^- with specific selectivity. Thus, **SPQ5** could act as Hg^{2+} and CN^- controlled “on-off-on” fluorescent chemosensor. The repeated switching behavior when altering adding amounts of Hg^{2+} and CN^- into the solution of **SPQ5**, evidently proved the excellent reusability and stability of **SPQ5** towards Hg^{2+} at least for three successive cycles (Fig. S14).

Scheme 2

In addition, we investigated the fluorescent “on-off-on” behavior mechanism, the ^1H NMR titration spectra were carried out. In the ^1H NMR titration spectra (Fig. S15), with the addition of Hg^{2+} , the significant downfield shift of resonance signals (H_{1-6}) on 8-hydroxyquinoline was observed. The results confirmed **SPQ5**- Hg^{2+} complex constructed by the coordination interaction of O and N with Hg^{2+} on the quinoline group [82]. The XRD spectra of **SPQ5**- Hg^{2+} showed no insignificant peaks (Fig. S17) also indicated that the **SPQ5** complexed with Hg^{2+} and π - π stacking between 8-hydroxyquinoline was destroyed. Meanwhile, C-H $\cdots\pi$ interaction of pillar[5]arene was broken, resulting in the solution of **SPQ5** fluorescence quenching (Scheme 2d). After addition of 4 equiv. of CN^- into **SPQ5**- Hg^{2+} , the 8-hydroxyquinoline hydrocarbon signals H_{1-6} have a significant upfield shift 0.06, 0.24, 0.34, 0.29, 0.18 and 0.18 ppm, respectively (Fig. S16). Indicating the formation of $\text{Hg}(\text{CN})_2$ complex between CN^- and Hg^{2+} . Meanwhile, both aryl hydrogen of Pillar[5]arene (Ha) and methylene bridge hydrogen (Hc) upfield shift 0.04ppm. Demonstrating that π - π stacking interactions of pillar[5]arene was recovered, which was shown in Scheme 2. We could also see this from XRD spectra (Fig. S17).

Fig. 5

To get deep insight into the morphological features of the powder **SPQ5**, SEM studies were carried out. As we could see in Fig. 6a, the images of **SPQ5** showed irregular block structure, when it was treated with DMF/ H_2O (8:2, v/v) binary solution, the morphology of **SPQ5** presented tight coralline structure (Fig. 2b),

indicating that the **SPQ5** self-assembled into two-dimensional supramolecular polymer chain, we also found that the **SPQ5** formed π - π stacking and C-H \cdots π interactions with the pillar[5]arene, leading to the formation of three dimensional supramolecular polymer networks. After adding Hg^{2+} into **SPQ5** (Fig. 6b), the tight coralline structure changed into lamellar structure means the formation of Hg^{2+} and quinolone coordination interaction resulting in the π - π stacking interactions between quinoline has been destruction. Otherwise, when **SPQ5**- Hg^{2+} was treated with CN^- (Fig. 6c), the image was transformed into a stick fiber structure due to the competitive complexation of CN^- to Hg^{2+} from **SPQ5**- Hg^{2+} coordination polymerization.

Fig. 6

The self-assembly process of chemosensor **SPQ5** with Hg^{2+} and CN^- was also investigated by the XRD patterns (Fig. S17). The XRD patterns obtained from DMF/ H_2O (8:2, v/v) binary solution of **SPQ5** clearly showed a typical diffraction peaks at $2\theta = 23.25^\circ$ and $2\theta = 24.15^\circ$ ($d = 3.82 \text{ \AA}$ and 3.68 \AA), indicating that π - π stacking interactions existed in the pillar[5]arene groups and 8-hydroxyquinoline groups (Scheme 2c). Otherwise, the in-significant peaks of **SPQ5**- Hg^{2+} indicated that π - π stacking was destroyed. What's more, the reappeared d-spacing of 3.83 \AA at $2\theta = 22.92^\circ$ means π - π stacking recovered when the CN^- was added into **SPQ5**- Hg^{2+} .

Since the fluorescence emission of **SPQ5** could be accurately controlled by alternative addition of Hg^{2+} and CN^- , the fluorescence emission of **SPQ5** could be defined as the logic gate output, which provides an entry for developing a supramolecular logic gate using Hg^{2+} (Input 1) and CN^- (Input 2) as two inputs. We

have designed a type of IMP logic gate (Fig. 7). For inputs, the addition and the absence of Hg^{2+} and CN^- could be defined as 1 and 0, respectively. For output, we defined the normalized fluorescence intensity of **SPQ5** turn on as “1” and turn off as “0”. Based on the above definitions, the fluorescence quenching of **SPQ5** is observed only in the addition of Hg^{2+} , so that the output is read as 0. Under other circumstances, the fluorescence of **SPQ5** is not quenched leading to the output being read as 1. From the truth table of Fig. 7a, it is observed that addition of only Hg^{2+} (Input1 = 1 and Input 2 = 0) causes a low fluorescence intensity value implying that the output signal is below the threshold value (output = 0). With other possible input combinations ((0, 0), (0, 1), and (1, 1)), the output signal is above the threshold value i.e. the output = 1. Hence, by monitoring the fluorescence intensity change of 1 at 410 nm by the two inputs (Hg^{2+} and CN^-); an IMP logic gate can be viewed.

Fig. 7

Moreover, in order to facilitate the applying of chemosensor **SPQ5**, the Hg^{2+} test kit was prepared by loading **SPQ5** on a silica gel plate (Fig. S18). The silica gel plate-based **SPQ5** test kit exhibits fascinating fluorescence emission, upon dipping the test kit into the different concentrations (from 1 M to 1×10^{-8} M) of Hg^{2+} aqueous solutions, distinct levels of brilliant fluorescence emission appeared under UV lamp. Therefore, the **SPQ5** based silica gel plates could act as a novel and efficient test kit for convenient detection of Hg^{2+} with high sensitivity.

4. Conclusions

In summary, we have rationally designed and synthesized a novel

8-hydroxyquinoline functionalized pillar[5]arene (**SPQ5**). It shows blue AIE fluorescence in DMF/H₂O (8:2, v/v) binary solution by π - π stacking and C-H \cdots π interactions. Meanwhile, chemosensor **SPQ5** shows highly selective and sensitive fluorescence “on-off” behaviour toward Hg²⁺ over other cations. The in situ prepared **SPQ5**-Hg²⁺ complex exhibits high selectively and sensitively to CN⁻ over other anions through a complexation reaction. The detection limit of **SPQ5** for Hg²⁺ and CN⁻ are as low as 2.53×10^{-8} M and 7.71×10^{-8} M, respectively. Furthermore other anions and cations had little influence on the probing behaviour. Moreover, the fluorescence changes of **SPQ5** upon the addition of Hg²⁺ and CN⁻ were utilized as an IMP logic gate at the molecular level, using Hg²⁺ and CN⁻ as chemical inputs and the fluorescence intensity signal as the output. Notably, the actual usage of chemosensor **SPQ5** was further demonstrated by test kits and silica gel plates which could convenient and efficient detect toxic Hg²⁺ in aqueous media.

Conflicts of interest

There are no conflicts to declare.

Acknowledgements

This work was supported by the National Natural Science Foundation of China (NSFC) (Nos. 21662031; 21661028; 21574104) and the Program for Changjiang Scholars and Innovative Research Team in University of Ministry of Education of China (NO. IRT 15R56).

Note and references

- [1] P Samanta, A V Desai, S Sharma, P Chandra, S K Ghosh. Selective recognition of Hg^{2+} ion in water by a functionalized metal-organic framework (MOF) based chemodosimeter. *Inorg Chem* 2018;57:2360-2364.
- [2] Y X Feng, X L Shao, K L Huang, J J Tian, X H Mei, Y B Luo, W T Xu. Mercury nanoladders: a new method for DNA amplification, signal identification and their application in the detection of Hg(II) ions. *Chem Commun* 2018;54:8036-8039.
- [3] F Wang, L Wang, X Q Chen, J Y Yoon. Recent progress in the development of fluorometric and colorimetric chemosensors for detection of cyanide ions. *Chem Soc Rev* 2014;43:4312-4324.
- [4] T Mede, M Jäger, U S Schubert. “Chemistry-on-the-complex”: functional Ru^{II} polypyridyl-type sensitizers as divergent building blocks. *Chem Soc Rev* 2018;47:7577-7627.
- [5] M Dong, Y Peng, Y M Dong, N Tang, Y W Wang. A selective, colorimetric, and fluorescent chemodosimeter for relay recognition of fluoride and cyanide anions based on 1, 10-binaphthyl bcaffold. *Org Lett* 2012;14:130-133.
- [6] V K Gupta, N Mergu, L K Kumawat, A K Singha. A reversible fluorescence “off-on-off” chemosensor for sequential detection of aluminum and acetate/fluoride ions. *Talanta* 2015;144:80-89.
- [7] A F D Namor, I Abbas, H H Hammud. A new calix[4]pyrrole derivative and its anion (fluoride)/cation (mercury and silver) recognition. *J Phys Chem B* 2007;111:3098-3105.

- [8] Y T Yang, C X Yin, F J Huo, J B Chao, Y B Zhang. Highly selective relay recognition of hydrogen sulfide and Hg(II) by a commercially available fluorescent chemosensor and its application in bioimaging. *Sens. Actuators B* 2014;204:402-406.
- [9] K Liu, Y Zhang, T Zhou, X H Liu, B Chen, X Wang, X J Zhao, J Z Huo, Y J Wang, B L Zhu. Sequential recognition of Hg²⁺ and I⁻ based on a novel BODIPY-salen sensor. *Sens. Actuators B* 2017;253:1194-1198.
- [10] S Y Lee, J J Lee, K H Bok, J A Kim, S Y Kim, C Kim. A colorimetric chemosensor for the sequential recognition of mercury (II) and iodide in aqueous media. *Inorg Chem Commun* 2016;70:147-152.
- [11] X X Wu, Q F Niu, T D Li. A novel urea-based “turn-on” fluorescent sensor for detection of Fe³⁺/F⁻ ions with high selectivity and sensitivity. *Sens. Actuators B* 2016;222:714-720.
- [12] L He, C Liu, J H Xin. A novel turn-on colorimetric and fluorescent sensor for Fe³⁺ and Al³⁺ with solvent-dependent binding properties and its sequential response to carbonate. *Sens. Actuators B* 2015;213:181-187.
- [13] H G Lee, K B Kim, G J Park, Y J Na, H Y Jo, S A Lee, C Kim. An anthracene-based fluorescent sensor for sequential detection of zinc and copper ions. *Inorg Chem Commun* 2014;39:61-65.
- [14] J Ding, H Y Li, Y j Xie, Q Peng, Q Q Li, Z Li. Reaction-based conjugated polymer fluorescent probe for mercury(II): good sensing performance with “turn-on” signal output. *Polym Chem* 2017;8:2221-2226.
- [15] H Ju, D J Chang, S Kim, H Ryu, E Lee, I H Park, J H Jung, M Ikeda, Y Habata, S

S Lee. Cation-selective and anion-controlled fluorogenic behaviors of a benzothiazole-attached macrocycle that correlate with structural coordination modes. *Inorg Chem* 2016;55:7448-7456.

[16] J Y Yang, T Yang, X Y Wang, M L Chen, Y L Yu, J H Wang. Mercury speciation with fluorescent gold nanocluster as a probe. *Anal Chem* 2018;90:6945-6951.

[17] X Tang, Z Zhu, Y Wang, J Han, L Ni, H Q Zhang, J Li, Y L Mao. A cyanobiphenyl based fluorescent probe for rapid and specific detection of hypochlorite and its bio-imaging applications. *Sens. Actuators B* 2018;262:57-63.

[18] T Gao, X Z Cao, J Dong, Y Liu, W W Lv, C M Li, X P Feng, W B Zeng. A novel water soluble multifunctional fluorescent probe for highly sensitive and ultrafast detection of anionic surfactants and wash free imaging of gram-positive bacteria strains. *Dyes Pigm* 2017;143:436-443.

[19] L L Long, M Y Huang, N Wang, Y J Wu, K Wang, A H Gong, Z J Zhang, J L Sessler. A mitochondria-specific fluorescent probe for visualizing endogenous hydrogen cyanide fluctuations in neurons. *J Am Chem Soc* 2018;140:1870-1875.

[20] J Canoura, Z W Wang, H X Yu, O Alkhamis, F F Fu, Y Xiao. No structure-switching required: a generalizable exonuclease-mediated aptamer-based assay for small-molecule detection. *J Am Chem Soc* 2018;140:9961-9971.

[21] Y C Lin, C T Chen. Acridinium salt-based fluoride and acetate chromofluorescent probes: molecular insights into anion selectivity switching. *Org Lett* 2009;11:4858-4861.

[22] X Jiao, Y Li, J Niu, X Xie, X Wang, B Tang. Small-molecule fluorescent probes

for imaging and detection of reactive oxygen, nitrogen, and sulfur species in biological systems. *Anal Chem* 2018;90:533-555.

[23] D Wu, A C Sedgwick, T Gunnlaugsson, E U Akkaya, J Yoon, T D James. Fluorescent chemosensors: the past, present and future. *Chem Soc Rev* 2017;46:7105-7123.

[24] Z Z Dong, C Yang, K Vellaisamy, G D Li, C H Leung, D L Ma. Construction of a nano biosensor for cyanide anion detection and its application in environmental and biological systems. *ACS Sens* 2017;2:1517-1522.

[25] K Daware, R Shinde, R S Kalubarme, M Kasture, A Pandey, C Terashima, S W Gosavi. Development of optical sensing probe for Hg(II) ions detection in ground water using Au, hexanedithiol and rhodamine B nanocomposite system, *Sen. Actuators B* 2018;265:547-555.

[26] P Veerakumar, S M Chen, R Madhu, V Veeramani, C T Hung, S B Liu. Nickel nanoparticle-decorated porous carbons for highly active catalytic reduction of organic dyes and sensitive detection of Hg(II) ions. *ACS Appl Mater Interfaces* 2015;7:24810-24821.

[27] N Ratner, D Mandler. Electrochemical detection of low concentrations of mercury in water using gold nanoparticles. *Anal Chem* 2015;87:5148-5155.

[28] Y Feng, D yan Deng, L C Zhang, R Liu, Y Lv. LRET-based functional persistent luminescence nanoprobe for imaging and detection of cyanide ion. *Sen. Actuators B* 2019;279:189-196.

[29] L A Greenawald, G R Boss, J L Snyder, A Reeder, S Bell. Development of an

inexpensive RGB color sensor for the detection of hydrogen cyanide gas. *ACS Sens* 2017;2:1458-1466.

[30] L Chen, L W He, F Y Ma, W Liu, Y X Wang, M A Silver, L H Chen, L Zhu, D X Gui, J D Wu, Z F Chai, S Wang. Covalent organic framework functionalized with 8-hydroxyquinoline as a dual-mode fluorescent and colorimetric pH sensor. *ACS Appl Mater Interfaces* 2018;10:15364-15368.

[31] J H Lee, Y H Lee, D C Choo, T W Kim. Color switching behaviors of organic bistable light-emitting devices fabricated utilizing an aluminum-nanoparticle-embedded tris(8-hydroxyquinoline)aluminum layer and double emitting layers. *Org Electron* 2017;50:94-99.

[32] Y Y Fang, C X Li, L Wu, B Bai, X Li, Y M Jia, W Feng, L H Yuan, A non-symmetric pillar[5]arene based on triazolelinked 8-oxyquinolines as a sequential sensor for thorium(IV) followed by fluoride ions. *Dalton Trans*, 2015,44:14584-14588.

[33] A N Kursunlu, Y Acikbas, M Ozmen, M Erdoganc, R, Capanc. Preparation of pillar[5]arene-quinoline Langmuir-Blodgett thin films for detection of volatile organic compounds with host-guest principles. *Analyst* 2017,142:3689-3698.

[34] W Zheng, G Yang, S T Jiang, N Shao, G Q Yin, L Xu, X Li, G Chen, H B Yang. A tetraphenylethylene (TPE)-based supra-amphiphilic organoplatinum (II) metallacycle and its self-assembly behavior. *Mater Chem Front* 2017;1:1823-1828.

[35] J Mei, Y Huang, H Tian. Progress and trends in AIE-based bioprobes: a brief overview. *ACS Appl Mater Interfaces* 2018;10:12217-12261.

- [36] D D La, S V Bhosale, L A Jones, and S V Bhosale. Tetraphenylethylene-based AIE-active probes for sensing applications. *ACS Appl Mater Interfaces* 2018;10:12189-12216.
- [37] M Gao and B Z Tang. Fluorescent sensors based on Aggregation-Induced Emission: recent advances and Perspectives. *ACS Sens* 2017;2:1382-1399.
- [38] T Takeda, S Yamamoto, M Mitsuishi, T Akutagawa. Thermoresponsive amphipathic fluorescent organic liquid. *J Phys Chem C* 2018;122:9593-9598.
- [39] H B Wang, G Y Liu. Advances in luminescent materials with aggregation-induced emission (AIE) properties for biomedical applications. *J Mater Chem B* 2018;6:4029-4042.
- [40] Q Wan, R Jiang, L L Guo, S X Yu, M Y Liu, J W Tian, G Q Liu, FJ Deng, X Y Zhang, Y Wei. Novel strategy toward AIE-active fluorescent polymeric nanoparticles from polysaccharides: preparation and cell imaging. *ACS Sustainable Chem Eng* 2017;5:9955-9964.
- [41] P F Zhang, Z Zhao, C S Li, H F Su, Y Y Wu, Ryan T K Kwok, J W Y Lam, P Gong, L T Cai, B Z Tang. Aptamer-decorated self-assembled aggregation-induced emission organic dots for cancer cell targeting and imaging. *Anal Chem* 2018;90:1063-1067.
- [42] Y Chen, X Min, X Zhang, F Zhang, S Lu, L P Xu, X Lou, F Xia, X, Zhang, S.Wang. AIE-based superwetttable microchips for evaporation and aggregation induced fluorescence enhancement biosensing. *Biosens Bioelectron* 2018;111:124-130.

- [43] Q L Zhao and J Z Sun. Red and near infrared emission materials with AIE characteristics. *J Mater Chem C* 2016;4:10588-10609.
- [44] N W Sun, K X Su, Z W Zhou, Ye Yu, X Z Tian, D M Wang, X G Zhao, H W Zhou and C H Chen. AIE-active polyamide containing diphenylamine-TPE moiety with superior electrofluorochromic performance. *ACS Appl Mater Interfaces* 2018;10:16105-16112.
- [45] H Nie, K Hu, Y J Cai, Q Peng, Z J Zhao, R R Hu, J W Chen, S J Su, A J Qin, B Z Tang. Tetraphenylfuran: aggregation-induced emission or aggregation-caused quenching. *Mater Chem Front* 2017;1:1125-1129.
- [46] M Wang, Y Xu, Y Liu, K Gu, J Tan, P Shi, D Yang, Z Guo, W Zhu, X Guo, M A C Stuart. Morphology tuning of aggregation-induced emission probes by flash nanoprecipitation: shape and size effects on in vivo imaging. *ACS Appl Mater Interfaces* 2018;10:25186-25193.
- [47] C Y Li, X L Liu, S S He, Y B Huang, D M Cui. Synthesis and AIE properties of PEG-PLA-PMPC based triblock amphiphilic biodegradable polymers. *Polym Chem* 2016;7:1121-1128.
- [48] C W Zhang, B Ou, S T Jiang, G Q Yin, L J Chen, L Xu, X Li, H B Yang. Cross-linked AIE supramolecular polymer gels with multiple stimuli-responsive behaviours constructed by hierarchical self-assembly. *Polym Chem* 2018;9:2021-2030.
- [49] X S Li, M J Jiang, J W Y Lam, B Z Tang, J N Y Qu. Mitochondrial imaging with combined fluorescence and stimulated raman scattering microscopy using a probe of

the aggregation induced emission characteristic. *J Am Chem Soc* 2017;139:17022-17030.

[50] Y X Chen, X H Min, X Q Zhang, F L Zhang, S M Lu, L P Xu, X D Lou, F Xia, X J Zhang, S T Wang. AIE-based superwetable microchips for evaporation and aggregation induced fluorescence enhancement biosensing. *Biosens Bioelectron* 2018;111:124-130.

[51] X J Feng, J H Peng, Z Xu, R R Fang, H R Zhang, X J Xu, L D Li, J H Gao, M S Wong. AIE-active fluorene derivatives for solution-processable nondoped blue organic light-emitting devices (OLEDs). *ACS Appl Mater Interfaces* 2015;7:28156-28165.

[52] L Y Wang, L Q Li, D R Cao. Synthesis, photoluminescence, chromogenic and fluorogenic discrimination of fluoride and cyanide based on a triphenylamine-tri(2-formyl BODIPY) conjugate. *Sens. Actuators B* 2017;241:1224-1234.

[53] J Zhao, Z H Chi, Y Zhang, Z Mao, Z Y Yang, E Ubba, Z G Chi. Recent progress in the mechanofluorochromism of cyanoethylene derivatives with aggregation-induced emission. *J Mater Chem C* 2018;6:6327-6353.

[54] P Gopikrishna, N Meher, P K Iyer. Functional 1,8-naphthalimide AIE/AIEEgens: recent advances and prospects. *ACS Appl Mater Interfaces* 2018;10:12081-12111.

[55] H Z Hu, F Y Wang, L S Yu, K K Sugimura, J P Zhou, Y Nishio. Synthesis of novel fluorescent cellulose derivatives and their applications in detection of nitroaromatic compounds. *ACS Sustainable Chem Eng* 2018;6:1436-1445.

- [56] S Pagidi, N K Kalluvettukuzhy, P Thilagar. Tunable self-assembly and aggregation-induced emission characteristics of triarylboron-decorated naphthalimides. *Organometallics* 2018;37:1900-1909.
- [57] T Ogoshi, T Yamagishi, Y Nakamoto. Pillar-Shaped macrocyclic hosts Pillar[n]arenes: new key players for supramolecular chemistry. *Chem Rev* 2016;116:7937-8002.
- [58] M A Kobaisi, S V Bhosale, K Latham, A M Raynor, S V Bhosale. Functional naphthalene diimides: synthesis, properties, and applications. *Chem Rev* 2016;116:11685-11796.
- [59] J Murray, K Kim, T Ogoshi, W Yao, B C Gibb. The aqueous supramolecular chemistry of cucurbit[n]urils, pillar[n]arenes and deep-cavity cavitands. *Chem Soc Rev* 2017;46:2479-2496.
- [60] T Kakuta, TA Yamagishi, T Ogoshi. Stimuli-responsive supramolecular assemblies constructed from pillar[n]arenes. *Acc Chem Res* 2018;51:1656-1666.
- [61] D Y Xia, L Y Wang, X Q Lv, J B Chao, X H Wei, P Wang. Dual-responsive [2]pseudorotaxane on the basis of a pH-sensitive pillar[5]arene and its application in the fabrication of metallosupramolecular polypseudorotaxane. *Macromolecules* 2018;51:2716-2722.
- [62] D Wu, Y Li, J Shen, Z Z Tong, Q L Hu, L P Lie, G C Yu. Supramolecular chemotherapeutic drug constructed from pillararene-based supramolecular amphiphile. *Chem Commun* 2018;54:8198-8201.
- [63] J P He, J Z Chen, S L Lin, D C Niu, J N Hao, X B Jia, N Li, J L Gu, Y S Li, J L

Shi. Synthesis of a pillar[5]arene-based polyrotaxane for enhancing the drug loading capacity of PCL-based supramolecular amphiphile as an excellent drug delivery platform. *Biomacromolecules* 2018;19:2923-2930.

[64] P Wei, S F Götz, S H Schubert, J C Brendel, U S Schubert. Accelerating the acidic degradation of a novel thermoresponsive polymer by host-guest interaction. *Polym Chem* 2018;9:2634-2642.

[65] Y Z Liu, YY Zhang, H T Z Zhu, H Wang, W Tian, B B Shi. A supramolecular hyperbranched polymer with multi-responsiveness constructed by pillar[5]arene-based host-guest recognition and its application in the breath figure method. *Mater Chem Front* 2018;2:1568-1573.

[66] L Shao, J Yang, B Hua. A dual-responsive cross-linked supramolecular polymer network gel: hierarchical supramolecular self-assembly driven by pillararene-based molecular recognition and metal–ligand interactions. *Polym Chem* 2018;9:1293-1297.

[67] P Wang, H Xing, D Y Xia, X F Ji. A novel supramolecular polymer gel constructed by crosslinking pillar[5]arene-based supramolecular polymers through metal-ligand interactions. *Chem Commun* 2015;51:17431.

[68] K C Jie, M Liu, Y J Zhou, M A Little, A Pulido, S Y Chong, A Stephenson, A R Hughes, F Sakakibara, T Ogoshi, F Blanc, G M Day, F H Huang, A I Cooper. Near-ideal xylene selectivity in adaptive molecular pillar[n]arene crystals. *J Am Chem Soc* 2018;140:6921-6930.

[69] C J Li, K Han, J Li, H C Zhang, J W Ma, X Y Shu, Z X Chen, L H Weng, X S Jia. Synthesis of pillar[5]arene dimers and their cooperative binding toward some neutral

guests. *Org Lett* 2012;14:42-45.

[70] K Wang, C Y Wang, Y Wang, H Li, C Y Bao, J Y Liu, S X Zhang, Y W Yang. Electrospun nanofibers and multi-responsive supramolecular assemblies constructed from a pillar[5]arene-based receptor. *Chem Commun* 2013;49:10528-10530.

[71] F Guo, Y Sun, B H Xi, G W Diao. Recent progress in the research on the host-guest chemistry of pillar[n]arenes. *Supramol Chem* 2018;30:81-92.

[72] Q Lin, X M Jiang, X Q Ma, J Liu, H Yao, Y M Zhang, T B Wei. Novel bispillar[5]arene-based AIEgen and its' application in mercury(II) detection. *Sen Actuators B* 2018;272:139-145.

[73] Q Lin, Y Q Fan, G F Gong, P P Mao, J Wang, X W Guan, J Liu, Y M Zhang, H Yao, T B Wei. Ultrasensitive detection of formaldehyde in gas and solutions by a catalyst preplaced sensor based on a Pillar[5]arene derivative. *ACS Sustainable Chem Eng* 2018;6:8775-8781.

[74] W J Qu, G T Yan, X L Ma, T B Wei, Q Lin, H Yao, Y M Zhang. "Cascade recognition" of Cu^{2+} and H_2PO_4^- with high sensitivity and selectivity in aqueous media based on the effect of ESIPT. *Sen. Actuators B* 2017;242:849-856.

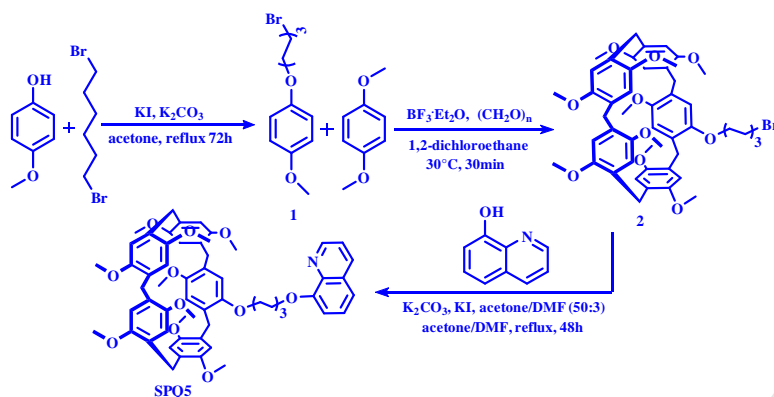
[75] J F Chen, Q Lin, Y M Zhang, H Yao, T B Wei. Pillararene-based fluorescent chemosensors: recent advances and perspectives. *Chem Commun* 2017;53:13296-13311.

[76] Q Lin, Y Q Fan, P P Mao, L Liu, J Liu, Y M Zhang, H Yao, T B Wei. Pillar[5]arene - based supramolecular organic framework with multi - guest detection and recyclable separation properties. *Chem Eur J* 2018;24:777-783.

- [77] Y M Zhang, W Zhu, W J Qu, K P Zhong, X P Chen, H Yao, T B Wei, Q Lin. Competition of cation- π and exo-wall π - π interactions: a novel approach to achieve ultrasensitive response. *Chem Commun* 2018;54:4549-4552.
- [78] Q. Lin, K. P. Zhong, J. H. Zhu, L. Ding, J. X. Su, H. Yao, T. B. Wei, Y. M. Zhang. Iodine controlled Pillar[5]arene-based multiresponsive supramolecular polymer for fluorescence detection of cyanide, mercury, and cysteine. *Macromolecules* 2017;50:7863-7871.
- [79] C Wei, B X Sun, Z L Cai, Z F Zhao, Y Tan, W B Yan, H B Wei, Z W Liu, Z Q Bian, C H Huang. Quantum yields over 80% achieved in luminescent europium complexes by employing diphenylphosphoryl tridentate ligands. *Inorg Chem* 2018;57:7512-7515.
- [80] J Orrego-Hernández, J Portilla. Synthesis of dicyanovinyl-substituted 1-(2-pyridyl)pyrazoles: design of a fluorescent chemosensor for selective recognition of cyanide. *J Org Chem* 2017;82:13376-13385.
- [81] A L Mirajkar, L L Mittapelli, G N Nawale, K R Gorea. Synthetic green fluorescent protein (GFP) chromophore analog for rapid, selective and sensitive detection of cyanide in water and in living cells. *Sens Actuators B* 2018;265:257-263.
- [82] G Q Chen, Z Guo, G M Zeng, L Tang. Fluorescent and colorimetric sensors for environmental mercury detection. *Analyst* 2015;140:5400-5443.

Table 1. Comparison of detection limit of sensor for Hg²⁺ with previously reported Hg²⁺ sensors

No.	Journal, Year, <i>Volume</i> , Page	Detection limit (M)
1	<i>Chem. Select</i> , 2018 , 3, 2088	1.7×10 ⁻⁶
2	<i>Anal. Chem.</i> , 2015 , 87, 5148	1.0×10 ⁻⁶
3	<i>Anal. Chem.</i> , 2014 , 86, 6843	5.0×10 ⁻⁸
4	<i>Sen. Actuators B</i> , 2018 , 269, 164	3.2×10 ⁻⁷
5	<i>Dyes Pigm</i> , 2019 , 163, 118	6.8×10 ⁻⁸
6	<i>Tetrahedron Lett</i> , 2017 , 58,4340	8.3×10 ⁻⁶
7	<i>J. Mater. Chem. A</i> , 2015 , 3, 13254	1.0×10 ⁻⁷
8	<i>Nanoscale</i> , 2017 , 9, 16728	8.0×10 ⁻⁸
9	<i>New J. Chem.</i> , 2017 , 41, 11533	4.6×10 ⁻⁷
10	<i>Anal. Chem.</i> , 2018 , 90, 5489	5.0×10 ⁻⁶
11	<i>Sen. Actuators B</i> , 2018 , 256, 528	9.8×10 ⁻⁸
12	<i>Talanta</i> , 2014 , 125, 322	2.8 × 10 ⁻⁶
13	<i>New J. Chem.</i> , 2015 , 39, 843	9.56 × 10 ⁻⁹
	This work	2.53×10 ⁻⁸



Scheme 1 Synthesis of the pillar[5]arene **SPQ5**.

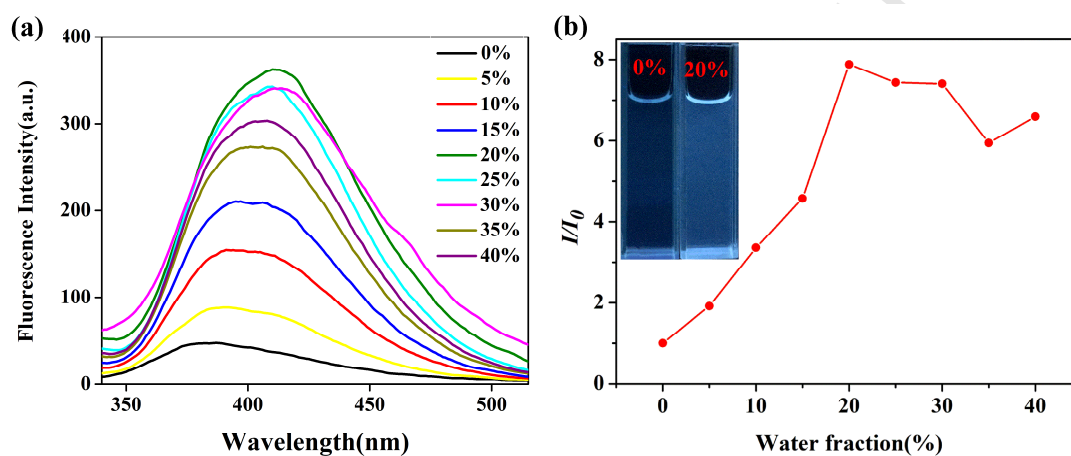


Fig. 1 (a) Fluorescence spectra of **SPQ5** in DMF/H₂O binary solution with different water fraction, solution concentration: 2.0×10^{-4} M ($\lambda_{\text{ex}} = 265$ nm); (b) Plot of relative emission intensity (I/I_0) values. I_0 = fluorescence intensity in pure DMF solution. Inset: photographs of **SPQ5** in DMF/H₂O binary solution (left: $f_w = 0\%$; right: $f_w = 20\%$) taken under 365 nm UV lamp.

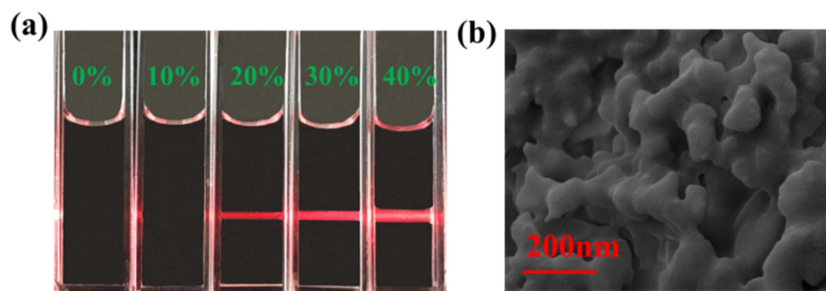


Fig. 2 (a). The Tyndall effect of **SPQ5** (2.0×10^{-4} M) with different volumetric fractions of water ($v_{\text{ol}}\%$); (b). SEM images of **SPQ5**.

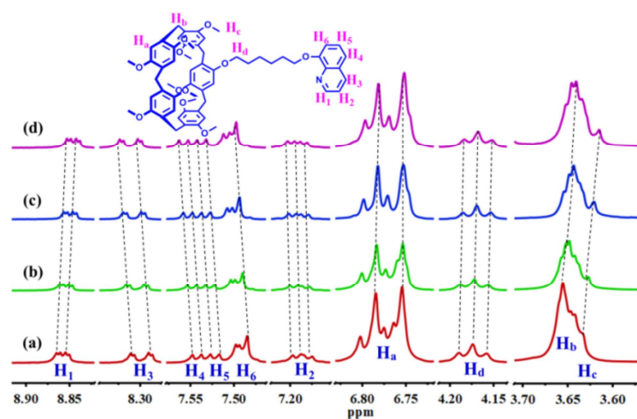


Fig. 3 Partial ^1H NMR titration spectra of **SPQ5** in $\text{DMSO-}d_6$ solution with different amount of H_2O (a) 0%; (b) 5%; (c) 10%; (d) 15%.

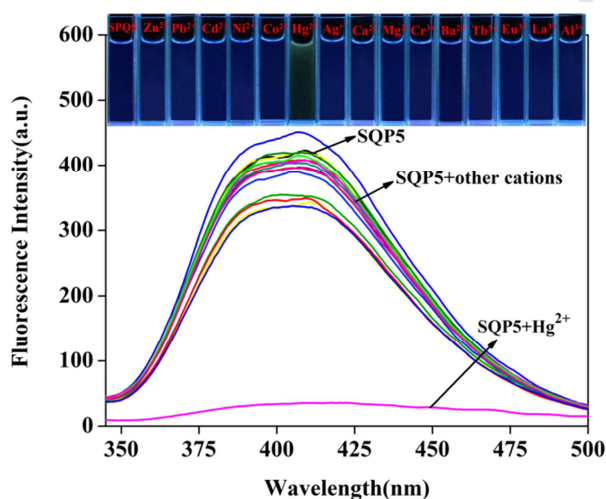


Fig. 4 Fluorescence emission ($\lambda_{\text{ex}} = 410 \text{ nm}$) spectra of **SPQ5** (20 mM) with metal ions (Zn^{2+} , Pb^{2+} , Cd^{2+} , Ni^{2+} , Co^{2+} , Hg^{2+} , Ag^+ , Ca^{2+} , Mg^{2+} , Cr^{3+} , Ba^{2+} , Tb^{3+} , Eu^{3+} , La^{3+} and Al^{3+}) in the $\text{DMF}/\text{H}_2\text{O}$ (8:2, v/v) binary solution in response to Hg^{2+} (2.0 equiv.). Inset: fluorescence color changes of **SPQ5** with various cations under UV lamp.

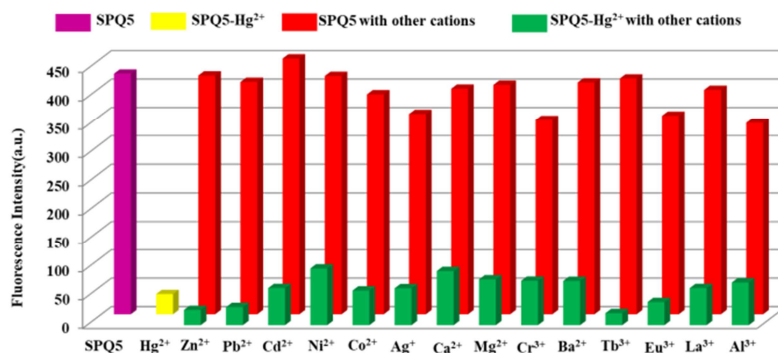
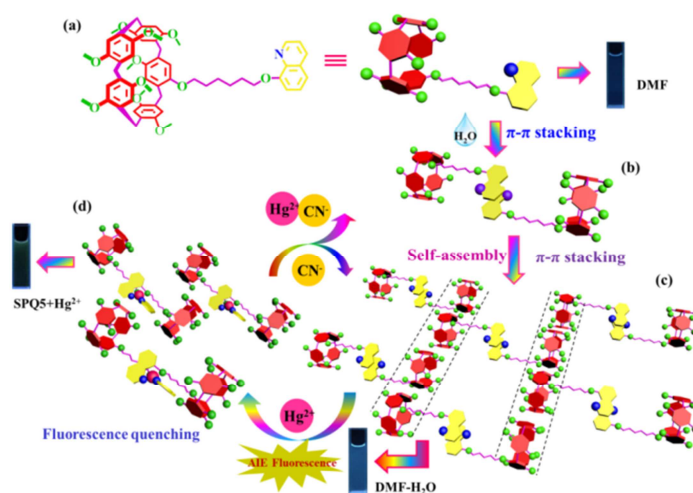


Fig. 5 Fluorescence response of **SPQ5** (2.0×10^{-4} M) in the presence of Hg^{2+} (2.0 equiv) and the addition of other metal ions (2.0 equiv) in DMF/ H_2O (8:2, v/v) binary solution. ($\lambda_{\text{ex}} = 265$ nm).



Scheme 2 (a) Molecular Structures of **SPQ5**. (b) Illustration of the formation of dimer structure with **SPQ5**. (c) Illustration of the Self-Assembly of **SPQ5** stacks into supramolecular networked. (d) Illustration of the formation of dimer structure with **SPQ5** and Hg^{2+} .

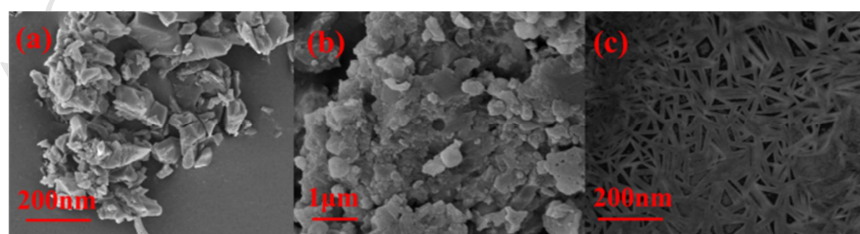


Fig. 6 SEM images of (a) **SPQ5**; (b) **SPQ5-Hg²⁺**; (c) **SPQ5-Hg²⁺-CN⁻**.

(a) Truth table

Input		Output
Hg ²⁺	CN ⁻	Fluorescence single
0	0	1
1	0	0
0	1	1
1	1	1

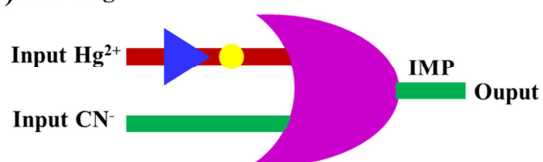
(b) Reading

Fig. 7 Implementation and truth table for IMP logic function using the sensor SPQ5.

Highlights

1. Synthesis of a novel 8-hydroxyquinoline functionalized pillar[5]arene (**SPQ5**).
2. The chemosensor **SPQ5** show pillar[5]arene-based AIE fluorescence.
3. The **SPQ5** could self-assemble by C-H $\cdots\pi$ interaction and $\pi\cdots\pi$ stacking interactions.
4. The **SPQ5** could highly selective and sensitive sequential detection of toxic Hg²⁺ and CN⁻.
5. **SPQ5**-based IMP logic gate sequential detection toxic Hg²⁺ and CN⁻ has been designed.